journal

J. Am. Ceram. Soc., 95 [7] 2178–2188 (2012)
DOI: 10.1111/j.1551-2916.2012.05186.x

Testing of Brushite ($CaHPO_4 \cdot 2H_2O$) in Synthetic Biomineralization Solutions and *In Situ* Crystallization of Brushite Micro-Granules

Matthew A. Miller,[‡] Matthew R. Kendall,[‡] Manoj K. Jain,[§] Preston R. Larson,[¶] Andrew S. Madden,[‡] and A. Cuneyt Tas[§,†,*]

[‡]School of Geology and Geophysics, University of Oklahoma, Norman, Oklahoma 73019

[§]College of Dentistry, University of Oklahoma Health Sciences Center, Oklahoma City, Oklahoma 73117

[¶]Samuel Roberts Noble Electron Microscopy Laboratory, University of Oklahoma, Norman, Oklahoma 73019

Conventional flat plate-shaped brushite, dicalcium phosphate dihydrate, $CaHPO_4 \cdot 2H_2O$), produced by reacting Ca-chloride and alkali phosphate salt solutions, were found to undergo a maturation process (changing their Ca/P molar ratio from 0.8 to the theoretical value of 1) similar to those seen in biological apatites. Water lily (WL)-shaped brushite crystals were produced in nonstirred aqueous solutions at room temperature in 24 h, by using precipitated calcite and $NH_4H_2PO_4$ as the starting chemicals. The hydrothermal transformation of WL-type brushite into octacalcium phosphate (OCP) or Ca-deficient hydroxyapatite (CDHA) was tested at 37°C by using four different biomineralization solutions, including Tris-buffered SBF (synthetic body fluid) and sodium lactate-buffered SBF solutions. All four solutions used in this study consumed the starting brushite in 1 week and caused transformation into a biphasic mixture of nanocrystalline OCP and CDHA of high surface area. WL-type brushite crystals when synthesized in the presence of small amounts of Zn^{2+} ions resulted in the formation of, for the first time, spherical micro-granules of brushite. Synthesis of brushite in spherical form was difficult prior to this study.

I. Introduction

BRUSHITE (DCPD, dicalcium phosphate dihydrate, $CaHPO_4 \cdot 2H_2O$), named after the American mineralogist George Jarvis Brush (1831–1912), is the predominant phase of the CaO–P_2O_5–H_2O system to precipitate between pH 2 and 6.5,[1–3] when Ca^{2+} and HPO_4^{2-} ions are brought together in an aqueous solution of this pH range. Brushite is mainly encountered in dental calculi, urinary stones and in chondrocalcinosis. It has a high solubility (pK_{SP} of 6.59 at 25°C) in comparison with the mineral of bone and teeth, hydroxyapatite, HA, $Ca_{10}(PO_4)_6(OH)_2$ (pK_{SP} of 116.8 at 25°C).[4] Its solubility is also significantly higher than that of octacalcium phosphate, OCP, $Ca_8(HPO_4)_2(PO_4)_4 \cdot 5H_2O$ (pK_{SP} of 96.6 at 25°C).[4]

Brushite is stable over the pH range 2–6.5, whereas OCP is stable from 5.5 to 7 and stoichiometric HA containing hydroxyl ions is stable over the neutral and basic pH range. Accordingly, brushite easily hydrolyzes to the more stable phases of OCP and apatite under physiological conditions.[5,6] Brushite powders reacted with an aqueous solution containing NaOH (or KOH), for instance, transforms to apatite within minutes.[7] The transformation of apatite into brushite was also studied.[8] The literature on the synthesis of brushite seems to be abundant, however, it focuses largely on the reaction of Ca^{2+} ions originating from highly soluble salts of Ca-chloride, Ca-nitrate or Ca-acetate with the aqueous HPO_4^{2-} ions (from ammonium- or alkali-phosphate salts). The encounter between the above ions causes instantaneous precipitation of flat plate (FP)- or lath-like crystals approximately 10–150 μm in length and 0.1–0.4 μm in thickness, depending on the solution's degree of supersaturation, pH, temperature and level of agitation.[9,10] Alternatively, reaction of phosphate ions with precipitated Ca-carbonate powder was shown to produce brushite with water lily (WL) or dumbbell morphology.[11]

High solubility of brushite, in comparison with apatite, led to the development of injectable paste formulations based on brushite [12–14] with β-TCP [β-tricalcium phosphate, β-$Ca_3(PO_4)_2$] as the starting material. Apelt *et al.* [15] reported in a comparative *in vivo* study that the TCP-containing brushite cements were rapidly biodegraded by macrophage activity and showed faster new bone formation compared with commercially available apatite cements. Therefore, the literature suggested that the *in vivo* performance of future scaffolds based on brushite could be higher than those based on nondegradable apatite.

Studies on the *in vitro*, acellular testing of brushite in synthetic biomineralization or calcification solutions, such as SBF (simulated/synthetic body fluid [16,17]) have been scarce.[11,18–26] While some of those [18–23] examined the transformation of brushite observed in electrochemically deposited calcium phosphates on titanium or in aqueous nucleation/crystallization on organic scaffolds, only a few of them [24–26] attempted studying pure brushite soaked in biomineralization solutions. The hydrothermal transformation of brushite powders having FP-type crystals was previously studied, at 37°C, in Tris-SBF solutions.[24] A recent study by Boccaccini *et al.* [27] disclosed that the Tris-buffer present in the conventional SBF solutions was able to cause an increased dissolution of the surface constituents of soaked bioglass and glass-ceramics samples and therefore led to the premature crystallization of apatite on sample surfaces, largely interfering with the reliability of so called bioactivity measurements based on such SBF solutions.

Moreover, research on the synthesis of brushite in aqueous media containing biologically significant elements (such as zinc) was also quite limited.[3,6,28–31] Zinc is found in the body in small amounts in almost all tissues, however, the bones and teeth store slightly higher amounts than others. Human blood plasma also contains approximately 1.5×10^{-2} m*M* zinc.[32] Zinc is an essential trace element in a variety of cellular processes including DNA synthesis, behavioral responses, reproduction and virility, bone formation, bone growth and

S. Bose—contributing editor

Manuscript No. 30448. Received October 10, 2011; approved March 07, 2012.
*Member, The American Ceramic Society
†Author to whom correspondence should be addressed. e-mail: c_tas@hotmail.com

wound healing.[33] The necessity of this trace element for bone growth was demonstrated by the observation that normal bone growth was retarded in animals that are zinc-deficient,[34] and the addition of zinc to these deficient diets resulted in a stimulation of both bone growth and mineralization.[35] Research literature related to brushite synthesized in the presence of zinc is hard to find.

The current study was designed to investigate the following questions.

1. Would brushite powders with the WL morphology soaked at 37°C (a) in Tris-buffered SBF solutions,[36] (b) in Lactic acid/Na-lactate-buffered SBF solutions[37] or (c) in synthetic biomineralization media [26] mimicking the electrolyte portion of one of the most common cell culture solutions (i.e., DMEM, Dulbecco's Modified Eagle Medium), display different or the same transformation products and release of acid?
2. How would Zn^{2+} ions added at small concentrations to the WL-type brushite synthesis solutions affect the morphology of brushite crystals?

II. Experimental Procedure

The starting chemicals of calcium carbonate ($CaCO_3$, calcite, Fisher Scientific, Fair Lawn, NJ, Catalogue No: C-63), ammonium dihydrogen phosphate ($NH_4H_2PO_4$, Fisher Scientific, No: A-684), sodium dihydrogen phosphate monohydrate ($NaH_2PO_4{\cdot}H_2O$, Merck, Darmstadt, Germany, No: SX-0710), calcium chloride dihydrate ($CaCl_2{\cdot}2H_2O$, Fisher Scientific, No: C-79), zinc chloride anhydrous ($ZnCl_2$, Merck, No: ZX-0065), magnesium chloride hexahydrate ($MgCl_2{\cdot}6H_2O$, Fisher Scientific, No: AC-19753), sodium chloride (NaCl, Sigma, St Louis, MO, No: S9888), potassium chloride (KCl, Sigma, No: P3911), sodium sulphate (Na_2SO_4, Fisher Scientific, No: AC-21875), sodium bicarbonate ($NaHCO_3$, Fisher Scientific, No: S233), disodium hydrogen phosphate (Na_2HPO_4, Fisher Scientific, No: S374), potassium dihydrogen phosphate (KH_2PO_4, Sigma, No: P0662), hydrochloric acid (HCl, VWR, Radnor, PA, No: VW3110), sodium lactate ($NaCH_3CH(OH)COO$, Sigma, No: L7022), lactic acid (1 *M*, Fluka, St. Louis, MO, No: 35202) and tris(hydroxymethyl) aminomethane [$(HOCH_2)_3CNH_2$, Sigma, No: 252859] were used in this study. Testing and crystallization experiments were performed in clean glass bottles by using freshly prepared deionized water (18.2 MΩ).

The procedure used to synthesize FP-shaped brushite crystals consisted of preparing two solutions.[11,24] Solution A was prepared as follows: 0.825 g of KH_2PO_4 was dissolved in 700 mL of deionized water, followed by the addition of 3.013 g of Na_2HPO_4. Solution B was prepared by dissolving 4.014 g of $CaCl_2{\cdot}2H_2O$ in 200 mL of water. Solution B was then rapidly added to solution A and the precipitates formed were aged for either 80 min, 4 h or 24 h at room temperature (RT, 22 ± 1°C), by continuous stirring at 300 rpm. Solids recovered by filtration (and follow-up washing with water) were dried overnight at 37°C. These samples are not included in Table I.

The WL brushite was produced using a different procedure. Ten grams of $NH_4H_2PO_4$, equal to 8.6936×10^{-2} mol P, was dissolved (by stirring with a magnetic Teflon-coated fish) in 85 mL of deionized water in a 125 mL-capacity glass bottle, followed by the addition of 2.0 g of $CaCO_3$ as calcite (1.9983×10^{-2} mol Ca^{2+}) powder. The calcite powder of this study is also known as the precipitated $CaCO_3$ or precipitated chalk, which is also used in toothpaste formulations. The bottle was screw capped and the formed suspension was shaken for only a few minutes to facilitate the complete soaking of the $CaCO_3$ particle surfaces with the phosphate solution. The bottle was then kept perfectly static for 24 h at RT. WL-type crystals were separated from their mother liquor by filtration (Whatman No. 4 paper), washed with 300 mL of water and dried at 37°C overnight. These are labelled as Sample-1 in Table I. To check the influence of ammonium ions on the morphology of crystals obtained in sample-1, sample-2 (of Table I) was prepared by using 11.997 g of $NaH_2PO_4{\cdot}H_2O$, which was again equal to 8.6936×10^{-2} mol of P.

To synthesize brushite crystals in the presence of aqueous Zn^{2+} ions in static suspensions similar to the above, we first prepared a stock solution of $ZnCl_2$ dissolved in water (i.e., 1.00 g $ZnCl_2$ in 100 mL of deionized water). In this study, 0.05–6 mL aliquots of this Zn stock solution were added to the above synthesis solutions which used $CaCO_3$ as the calcium source. The preparation conditions for the select samples of the brushite crystallization study are given in Table I. The nominal Zn^{2+} (from the $ZnCl_2$ solution added) to Ca^{2+} (from $CaCO_3$) molar ratio was given in the last column of Table I. Each crystallization run was repeated at least three times and the morphology of the brushite crystals was monitored by using an optical microscope (Olympus, IX-71, Tokyo, Japan).

Four different biomineralization solutions were used in this study, whose compositions are given in Table II. The numbers in Table II denoted the amounts of chemicals added (in grams, except otherwise indicated) to 1 L of water to prepare the solutions. These solutions were stored in 1 L-capacity clean glass bottles in a refrigerator (+4°C) when they were not in use. All four solutions had a pH value of 7.4 when prepared, similar to the electrolyte portion of blood plasma. BM-7,[26] *Tris*-SBF[17,36] and *Lac*-SBF [37] had a Ca/P molar ratio of 2.50, whereas the BM-3 [26] solution had a Ca/P molar ratio of 1.99 similar to that of DMEM solutions. *Lac*-SBF solution perfectly matches the ion concentrations of blood plasma.

The biomineralization solutions were used to monitor the phase changes to occur in the brushite powders. One gram portions of brushite powders were placed in a glass bottle, followed by adding 100 mL of the specific solution. The bottles were kept static in a 37°C oven. The solutions were totally replenished (with an unused solution) every 24 h. Solids recovered at the end of the specified aging times were filtered, washed with water and dried at 30°C.

Samples were characterized by scanning electron microscopy (SEM, JEOL JSM-840A, Tokyo, Japan), energy disper-

Table I. Sample Preparation

Sample	Water (mL)	$NH_4H_2PO_4$ (g)	$NaH_2PO_4{\cdot}H_2O$ (g)	$CaCO_3$ (g)	$ZnCl_2$ sol^n (mL)	Zn/Ca molar ratio
1	85	10.00	–	2.00	–	–
2	85	–	11.997	2.00	–	–
3	84.5	10.00	–	2.00	0.05	1.836×10^{-3}
4	84	10.00	–	2.00	1	3.672×10^{-3}
5	83	10.00	–	2.00	2	7.343×10^{-3}
6	82.5	10.00	–	2.00	2.5	9.179×10^{-3}
7	82	10.00	–	2.00	3	1.101×10^{-2}
8	81	10.00	–	2.00	4	1.469×10^{-2}

Table II. Preparation of Biomineralization Solutions

Chemical	BM-3 [26]	BM-7 [26]	*Lac*-SBF[37]	*Tris*-SBF [17,36]
NaCl	4.7865	4.7865	5.2599	6.5456
KCl	0.3975	0.3975	0.3730	0.3730
$MgCl_2{\cdot}6H_2O$	0.1655	0.1655	0.3049	0.3049
$CaCl_2{\cdot}2H_2O$	0.2646	0.3330	0.3675	0.3675
$NaHCO_3$	3.7005	3.7005	2.2682	2.2682
$NaH_2PO_4{\cdot}H_2O$	0.1250	0.1250	–	–
Na_2HPO_4	–	–	0.1419	0.1419
Na_2SO_4	–	–	0.0710	0.0710
Tris	–	–	–	6.0570
1 *M* HCl	–	–	–	40 mL
Na-lactate	–	–	2.4658	–
1 *M* lactic acid	–	–	1.5 mL	–
Ca/P molar ratio	*1.99*	*2.50*	*2.50*	*2.50*

sive x-ray spectroscopy [EDXS, Kevex; Thermo Scientific (Scotts Valley, CA) detector with iXRF System interface +EDS2008 software, Houston, TX], surface area measurements (BET, Brunauer-Emmett-Teller, Quantachrome Nova 2000e, Boynton Beach, FL) and powder x-ray diffraction (XRD, Ultima IV, Rigaku, Tokyo, Japan). SEM and EDXS samples were sputter-coated with a thin layer of Au-Pd alloy prior to imaging. Surface areas of powder samples were determined by five-point BET analysis of the nitrogen adsorption isotherm, obtained at −196°C after degassing overnight at 30°C (Quantachrome Nova 2000e, Boynton Beach, FL). Samples for XRD runs were first ground in a mortar by using a pestle. All the XRD scans ($\lambda = 1.5406$ Å) were performed in variable slit mode, with an irradiated area of 17 mm^2, a receiving slit of 0.3 mm and a divergence height limiting slit of 10 mm. The scan range for each XRD sample was from 4 to 40° 2θ, with a step size of 0.02° and a 3 s count time on a rotating specimen holder.

III. Results and Discussion

This study originated from an unprecedented observation about the FP-shaped conventional brushite crystals which we synthesized according to the recipe given in the Experimental Procedure section. Brushite crystals went through a process of maturation as a function of aging time in their mother liquors, i.e., their Ca/P molar ratio increased with time, eventually converging to unity. The inset in Fig. 1(a) depicted the semiquantitative EDXS-determined Ca/P molar ratio of brushite crystals as a function of time in the synthesis solution. The SEM morphology [Fig. 1(b)] and XRD trace of the crystals did not show any difference with respect to the aging time, either 80 min, 4 h or 24 h. The BET surface area of FP-brushite powders stirred for 4 h at RT in their synthesis solutions was measured to be 1.65 ± 0.1 m^2/g.

Such maturation processes are not uncommon in calcium phosphate phases, especially the amorphous or cryptocrystalline (so called poorly crystalline) calcium phosphates/apatites, as seen in new bones.[38] To the best of our knowledge, this will be the first study to report the maturation of brushite powders. Brushite contains water incorporated in its crystal structure and these water layers appear as bilayers parallel to the (020) faces of crystals.[39,40] Water molecules inside the crystal structure are linked to the HPO_4^{2-} groups by bulk hydrogen bonds, but these hydrogen bonds are broken when the bilayers of water molecules were interrupted by the crystal surface termination (as clearly shown in Fig. 1 of Ref. 39). We therefore hypothesize that the maturation phenomena exhibited by the brushite crystals was due to the necessity of reaching a thermodynamic equilibrium in the synthesis solutions for these water bilayers to sandwich in between a significant number of HPO_4^{2-} and Ca^{2+} ions, according to the brushite crystal structure. As direct hydrogen bonds shall exist

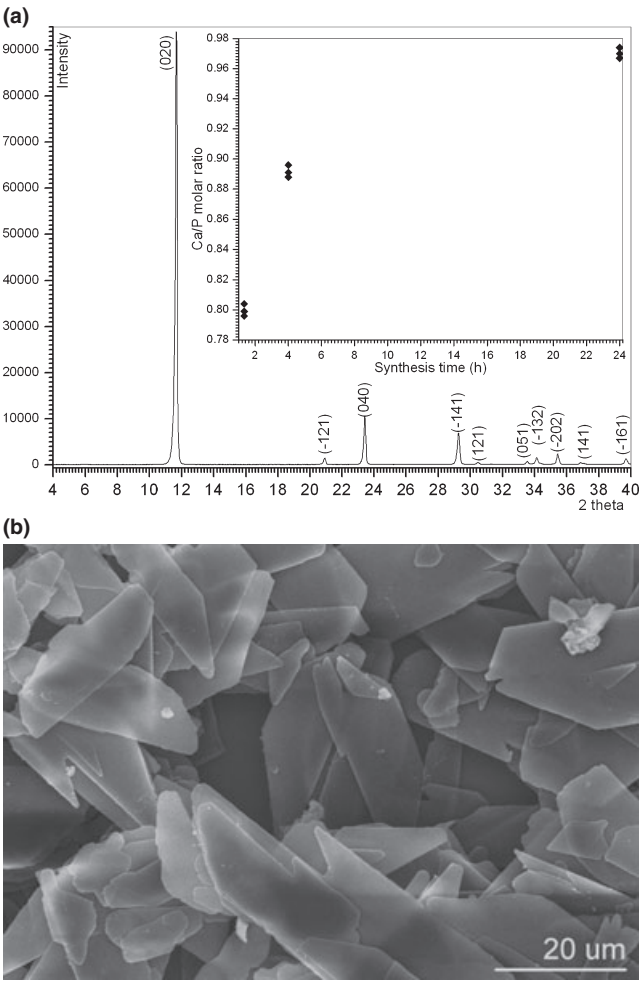

Fig. 1. (a) XRD and EDXS data of flat plate (FP)-type brushite. (b) SEM photomicrograph of flat plate (FP)-type brushite (80 min sample).

(in the bulk of the crystal, away from the surface) between the water bilayers and HPO_4^{2-} ions but not with Ca^{2+} ions, this may lead to an initial Ca-deficiency in the formed crystals. Our Fig. 1(a), with the help of EDXS data, revealed this initial Ca-deficiency in brushite for the first time, which drastically decreased with an increase in the aging time in the mother liquors.

Under the light of the above-mentioned observation, we slightly changed the way we planned to synthesize the brushite crystals to be used in the biomineralization solution testing part of this study. We had previously developed a new way of synthesizing WL-shaped (instead of flat plate FP-shaped) brushite crystals [25] by reacting precipitated $CaCO_3$(s) in stirred aqueous solutions of $NH_4H_2PO_4$, however, in that previous study the formed crystals were separated from their mother solutions quite prematurely, after 30 min. Therefore, in the current study the time-of-stay in the mother solution was increased to 24 h. Each sample was checked for the Ca/P molar ratio by using EDXS. The FP-shaped brushite crystals (and their synthesis technique) were not used in this study after it provided the seed information.

Figures 2(a) and (b) showed the XRD trace and the SEM photomicrographs of sample-1 of Table I respectively. The WL-shaped brushite crystals were about 100 μm in length and their XRD data conformed to the ICDD PDF 9-0077 standard pattern.[41] One of the intense XRD peaks of WL-type brushite is observed at 29.21°2θ [Fig. 2(a)] and the major peak of calcite is expected to be seen at 29.41°2θ (ICDD PDF 5-0586), which may be regarded as a close overlap. However, the next strong peak of calcite is located at

39.41°2θ and this one does not pose an overlap with any of the peaks of the brushite phase. The low intensity peak detected at 39.4°2θ in Fig. 2(a) could well correspond to the calcite phase, which accounts for the unreacted $CaCO_3$ in the static, nonagitated crystallization runs of this study.

The EDXS analysis performed on sample-1 yielded a Ca/P molar ratio of 0.98 ± 0.03. This method of synthesizing brushite crystals always resulted in the reduction in the extraordinary intensity of the (020) reflection of FP-shaped brushite [as shown in Fig. 1(a)]. WL-type brushite crystals are more intergrown, which helped to obtain a more disorientated distribution of smaller crystal plates and reduce the preferred orientation effects dominantly observed in the XRD spectra of FP-type brushite samples.

The BET surface area of sample-1 powders was found to be 0.37 m^2/g. Conventional FP-type brushite powders consisted of quite thin and fragile FPs [Fig. 1(b)]. Such thin plates of brushite are not even resistant to the mechanical loads exerted during the spatula mixing of these FP powders together with other calcium phosphates, such as cryptocrystalline carbonated apatite or α-TCP powders, in self-setting calcium phosphate bone cement applications. The WL-type brushite powders (as in sample-1), in stark contrast to FP-type brushite, were found to retain their particle morphology even after light grinding with an agate pestle in an agate mortar. The smaller surface area of WL-type brushite (in comparison with that of FP) may also be beneficial for the minimization of the volume of setting solution/liquid needed in bone cement applications,[42] when such brushite powders are to be used as one of the constituents of the powder component of a bone cement or putty.

The following question arose at this point. Is this morphology of brushite shown in Fig. 2(b) due to the ammonium ions in the synthesis solutions? To answer that experimentally, $NH_4H_2PO_4$ was completely replaced by $NaH_2PO_4{\cdot}H_2O$ in a number of experiments (e.g., sample-2 of Table I), by keeping the nominal Ca/P molar ratio in the solutions of sample-1 and sample-2 exactly the same. The answer was decisive; ammonium ions did not cause this change in morphology (from conventional FPs to WL), and XRD data in comparison with those of the FP-shaped brushite synthesis practises.[24] The XRD and SEM data [of Figs. 3(a) and (b)] of both samples 1 and 2 were found to be identical. Na^+ is a large monovalent cation similar to NH_4^+, but with a greater ionic potential. If specific interactions between the monovalent cations and the growing crystal significantly influenced crystal growth, it would be expected that Na^+ would have a greater effect. The lack of a noticeable change illustrates that the monovalent cations served as spectator ions in the crystal growth process.

Interestingly, the brushite crystal morphology depicted in Figs. 2(b) and 3(b) resembled very much those obtained in the electrochemical deposition of brushite onto titanium or titanium alloy cathodes.[23,43–47] The precipitate-free and acidic (of pH around 4) electrolytes used in the electrochemical deposition processes [23,43–47] typically utilized Ca-nitrate (or Ca-chloride), dissolved in water together with $NH_4H_2PO_4$ (or NaH_2PO_4). It is practically difficult to form a precipitate-free aqueous electrolyte by using Ca-nitrate (or -chloride) and $(NH_4)_2HPO_4$ (or Na_2HPO_4) because of the imminent precipitation of FP-shaped brushite at the moment of the encounter of Ca^{2+} and HPO_4^{2-} ions.[48,49] Therefore, the reason for the morphological similarity

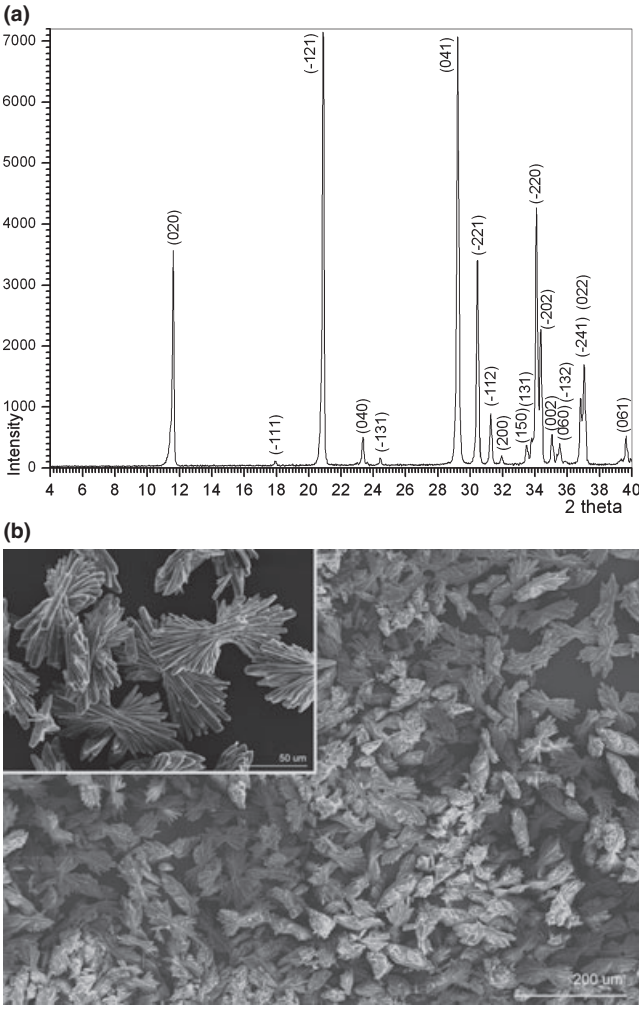

Fig. 2. (a) XRD and (b) SEM data of sample-1 of Table I.

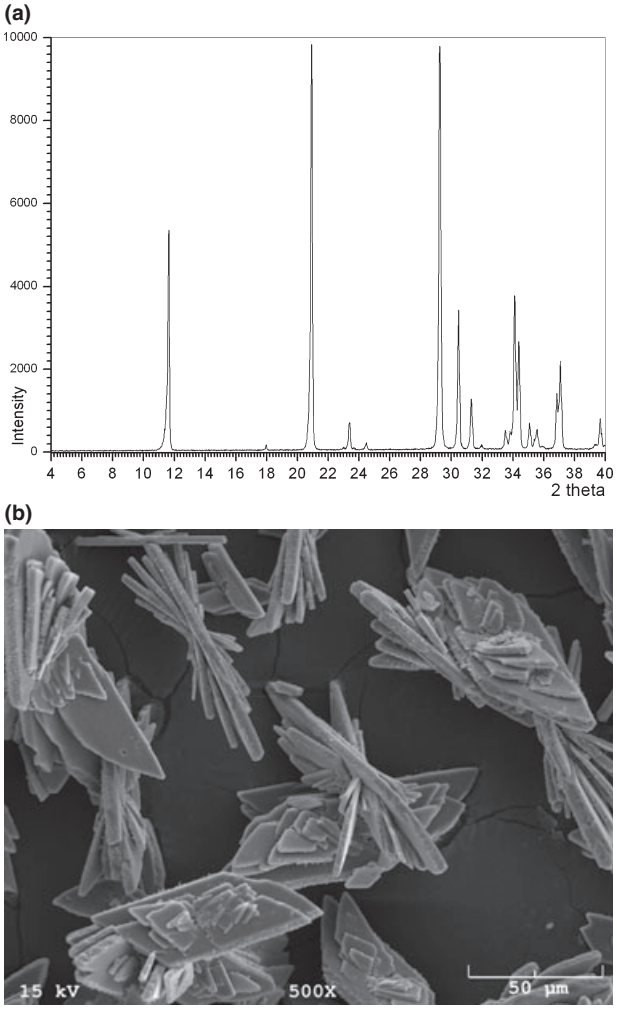

Fig. 3. (a) XRD and (b) SEM data of sample-2 of Table I.

of brushite crystals of the current study and those obtained in electrochemical deposition processes could be the use of $H_2PO_4^-$ ions.

The variation in the solution pH during the synthesis of sample-1 (Table I) is depicted in Fig. 4(a). The ammonium dihydrogen phosphate solution (10.0 g in 85 mL H_2O) was initially at pH 4.0 at RT, and at the moment of the addition of 2.00 g of precipitated calcite powder, it instantly rose to around 4.85. This is a non-agitated, static crystallization system, and within the next 15–16 min, the pH increased rather sharply to around 5.4, and after that moment the pH increase leveled off, and it took around 19–20 h for the solution pH to reach 5.7. The value of 5.72 ± 0.02 at the end of 24 h of RT aging was interestingly reproducible, and in every experiment the final pH of 5.70–5.74 was recorded. If one were adding 8.7 g of calcite powder (to adjust the Ca/P molar ratio in solution at 1) into the above-mentioned static-synthesis bottles, the solution pH values would be close to 7 and the recovered powders (after 24 h) would contain significant amounts of unreacted $CaCO_3$. This was why we fixed the Ca/P ratio at 0.23.

The entire reaction proceeded together with a slow CO_2(g) evolution in the form of bubbles rising to the solution surface from the solid phase at the bottom of reaction bottles. $CaCO_3$ of calcite form has a distinct dissolution rate dependence on the solution pH, as it rapidly decreases over the pH range 1.5–5 and then remains more or less constant over the pH range 5–9.[50–52] The dissolution rate of calcite at pH 5 is around 3×10^{-6} mol·m^{-2}·s^{-1}, whereas the same value for aragonite is about half of this, 1.3×10^{-6} mol·m^{-2}·s^{-1}.[50–52] To compare directly, the dissolution rate for brushite (in water) was reported by Tang *et al.* [53] to be 7.1×10^{-6} mol·m^{-2}·s^{-1} at pH 5.5 and RT. What happens within the first 15–16 min shown in Fig. 4(a) can best be explained by the below equations,[54] i.e., the affinity of $CaCO_3$ to steal a proton from the dissolved ammonium dihydrogen phosphate playing a key role;

$$CaCO_3(s) + NH_4^+(aq) + H_2PO_4^-(aq) \rightarrow CaHCO_3^+(aq) + NH_4^+(aq) + HPO_4^{2-}(aq) \quad (1a)$$

$$CaHCO_3^+(aq) + NH_4^+(aq) + HPO_4^{2-} \rightarrow CaHPO_4{\cdot}2H_2O(s) + NH_4^+(aq) + HCO_3^-(aq) \quad (1b)$$

According to the above model, ammonium ions were indeed spectator ions, and the release of the proton from $CaHCO_3^+$ did not result in a decrease in the solution pH as that proton was used in forming the bicarbonate ions. The rise in pH is likely due to the consumption of protons from the production of carbonic acid, evidence for which is given by the observation of exsolving CO_2(g). Release of CO_2(g) requires the double-protonation of carbonate ions, followed by the fast dehydration reaction. The next issue arising here is the high dissolution rate of brushite, which is 2.4 times higher than that of the precipitated calcite used in this study (which was fully characterized elsewhere [55]).

The precipitated calcite powder of this study consisted of submicron spindle-shaped particles and had a BET surface area of around 6 ± 0.3 m^2/g.[54,55] Precipitated calcite is typically produced by the carbonation process of $Ca(OH)_2$ slurries.[56]

If the solution pH in this crystallization system remains over the narrow range of 5.44–5.74 for about 24 h [see Fig. 4(a)] and if over this pH range brushite has a significant dissolution rate,[53] would it be possible to see at least some evidence of dissolution-reprecipitation processes on the formed brushite crystals? The answer was positive and almost all the high magnification SEM photomicrographs captured in this study were showing submicron spikes, nano-thick sheets or dissolution spots as the one reproduced in Fig. 4(b) (for the composition of sample-1).

The literature related to the testing of the *in vivo* behavior of brushite-based bone cements, [12–15] mentioned a slight inflammatory reaction observed within the first few days of implantation. This might be due to the release of acidic HPO_4^{2-} ions from brushite. One of the major impetuses of the current study was to search for *in vitro* testing procedures which could account for this initial acidity of brushite, without necessitating *in vivo* experimentation. To this purpose, the WL-type powders of sample-1 of this study were soaked in four different synthetic physiological fluids or biomineralization solutions (of Table II) which were designed to mimic the acellular, inorganic electrolyte portion of blood plasma, with or without using organic buffering agents. The *in vitro* testing of FP-type brushite powders were performed previously.[24] Figure 5 depicted the pH change in those four different biomineralization solutions as a function of brushite powder (WL, sample-1) aging time, and it was quite remarkable that all four solutions showed the minimum in pH value at the end of 2 d of soaking at 37°C. All four solutions then exhibited a gradual, but constant rise in solution pH from 3 to 7 d. It shall also be noted here that BM-3,[26] BM-7,[26] *Tris*-SBF [17,36] and *Lac*-SBF [37] solutions were all at pH 7.4 at the time of their preparation.

It should be noted that the *Tris*- and *Lac*-SBF solutions, which are buffered with Tris-HCl and sodium lactate-lactic acid pairs, respectively, did not exhibit a drop in solution pH after 24 h of soaking of the brushite powders at 37°C. On

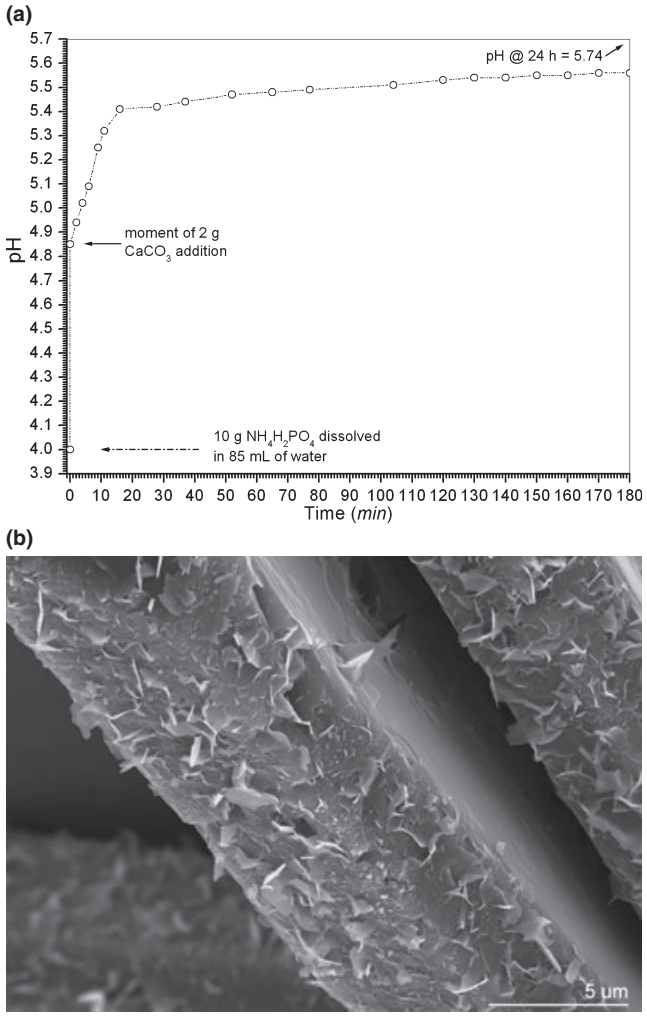

Fig. 4. (a) pH evolution during synthesis of sample-1 at RTand (b) SEM micrograph showing dissolution-reprecipitation phenomena on the edges of sample-1 crystals.

the other hand, BM-3 and BM-7 solutions, which are using the $HCO_3^-(aq)$-$CO_2(g)$ pair as the weak buffering agent (just like the human blood), were not able to maintain the solution pH at 7.4, even during the first 24 h. BM-3 solution (Ca/P = 1.99), devoid of any amino acids and vitamins, closely resembles the inorganic, electrolyte portion of DMEM cell culture solutions, whereas the BM-7 solution is very similar to the BM-3 solution except its Ca/P molar ratio of 2.50 exactly matches that of human blood.[26] BM-3 and BM-7 solutions do possess the apparent advantage of not containing any organic buffering agents (such as Tris, Hepes, lactate, etc.), which the human blood does not have as well.

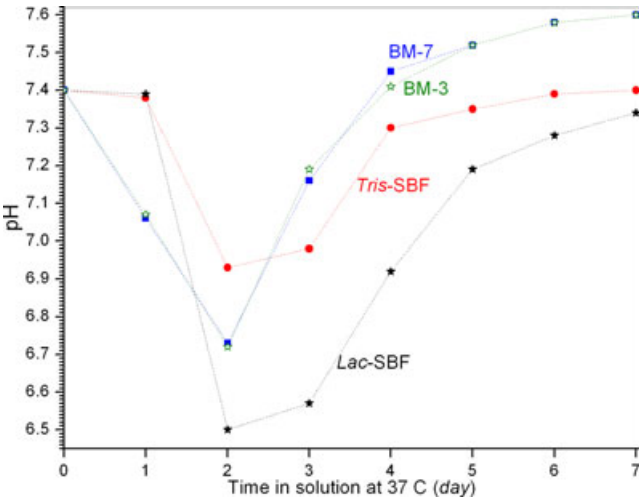

Fig. 5. pH evolution in testing sample-1 powders at 37°C in the biomineralization solutions.

Figures 6(a) through (d) display the powder XRD data of samples recovered from BM-3, BM-7, *Tris*-SBF and *Lac*-SBF solutions, at different time-points, following drying at 30°C. One-day samples separated from the BM-7, *Tris*-SBF and *Lac*-SBF solutions all showed that large portions of the brushite powders remained unreacted. However, there was a significant difference between the 1-d BM-7 sample and the 1-d samples of both SBF solutions, and the BM-7 sample contained higher amounts of cryptocrystalline (or nanocrystalline) OCP/apatitic calcium phosphate, indicated by the broad peaks observed at around 26 and 32°2θ in Fig. 6(a). In other words, the XRD traces of 1-d samples of brushite soaked in *Tris*- and *Lac*-SBF [Figs. 6(b) and (c)] were showing much less of an activity around the above-stated 2θ ranges.

BM-3 and BM-7 solutions produced almost the same pH versus soaking time data (Fig. 5), however, for the 2-d samples the pH of the Lac-SBF solution dropped to around 6.5, the pH value for the BM-3 and BM-7 solutions were around

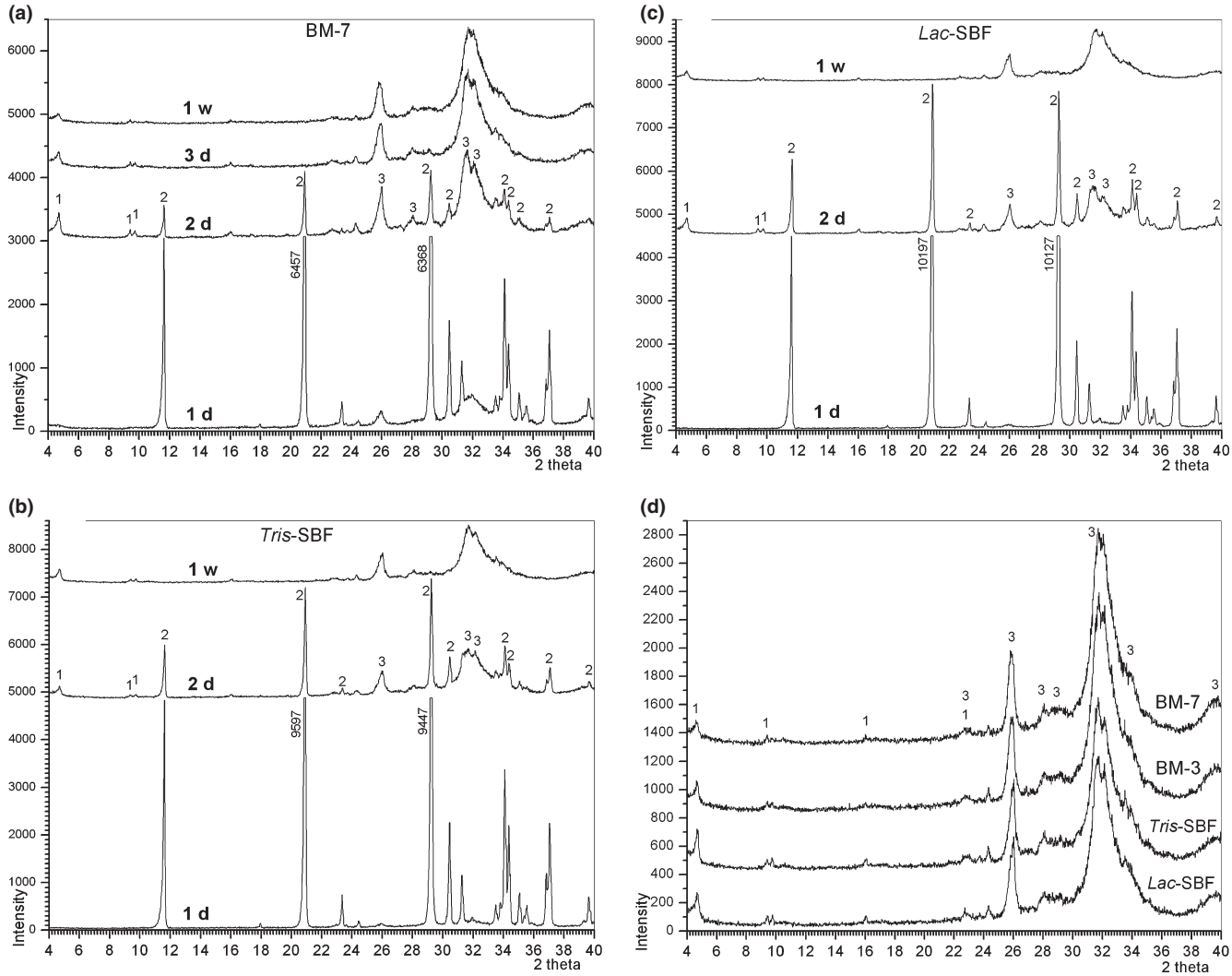

Fig. 6. XRD data of sample-1 soaked in (a) BM-7 solution, (b) *Tris*-SBF, (c) *Lac*-SBF for different periods at 37°C, (d) comparison of all samples after 1 week in the solutions indicated (time-points are indicated as 1 d, 2 d or 1 week; characteristic OCP peaks are denoted by 1, brushite peaks by 2 and CDHA peaks by 3; original intensities indicated on the cropped peaks).

6.75 and for the Tris-SBF solution the pH dropped to about 6.95. This meant that none of the solutions tested were able to exert its buffering capacity at the end of 2 d. This was expected as brushite is a soluble calcium phosphate (incomparable with hydroxyapatite), and it is releasing both Ca^{2+} and HPO_4^{2-} ions to the solutions it is soaked in. There was one common point in the XRD data of all the 2-day samples [Figs. 6(a), (b) and (c), i.e., they clearly showed the peaks of OCP ($Ca_8(HPO_4)_2(PO_4)_4{\cdot}5H_2O$)], together with a decreased amount of unreacted brushite. This further pH decrease in going from 1-d to 2-d samples (Fig. 5) can probably be explained by [6,26]

$$10CaHPO_4{\cdot}2H_2O \rightarrow Ca_8(HPO_4)_2(PO_4)_4{\cdot}5H_2O + 2Ca^{2+} + 4H_2PO_4^- + 15H_2O \quad (2)$$

$$6CaHPO_4{\cdot}2H_2O + 2Ca^{2+} \rightarrow Ca_8(HPO_4)_2(PO_4)_4{\cdot}5H_2O + 4H^+ + 7H_2O \quad (3)$$

It is apparent from the data of Fig. 5 that the *Lac*-SBF, BM-3 and BM-7 solutions were not able to buffer the H^+ and $H_2PO_4^-$ ions generated in Eqs. (2) and (3) as much as the *Tris*-SBF solution can, especially during the first 2 days of soaking. Equation (3) helps to explain the necessary presence of Ca^{2+} ions in the solutions to form OCP (Ca/P molar = 1.333) from brushite (Ca/P molar = 1.00).

The transformation or hydrolysis of OCP into CDHA (Ca-deficient hydroxyapatite, Ca/P molar = 1.50) can be expressed by

$$Ca_8(HPO_4)_2(PO_4)_4{\cdot}5H_2O + Ca^{2+} \rightarrow Ca_9(HPO_4)(PO_4)_5(OH) + 2H^+ + 4H_2O \quad (4)$$

Protons generated in Eq. (4) would help to explain why all the solutions of Fig. 5 struggled to raise the pH to the physiological level (7.4), by the 3rd day. The organic-free solutions BM-3 and BM-7, on the other hand, were able to raise the pH to the physiological level (7.4) at day 4 in Fig. 5. The XRD data of Fig. 6(d) compares the 1-week samples obtained from all solutions used in this study, i.e., BM-3, BM-7, *Tris*-SBF and *Lac*-SBF solutions, which clearly shows that the XRD traces of all the samples were almost identical and that all the samples did not contain any residual brushite.

In brief, all the 7th day samples (Fig. 5) obtained from four different biomineralization media unquestionably showed the presence of characteristic X-ray diffraction peaks for the OCP phase. When the OCP peaks are present in such biomimetically-produced calcium phosphate samples, it is not quite possible to claim that those broad peaks observed at 26° 2θ, and between 30° and 35° 2θ could only belong to apatitic calcium phosphate, as they also belong to the OCP phase, especially if it is nanocrystalline. The best thing one could claim in this case would be the equilibrium described by Eq. (4) above, i.e., a two-phase mixture of OCP and CDHA. The above data [Figs. 6(a) through (d)] pointed out the coexistence of brushite and OCP (1st and 2nd time-points), then to the disappearance of brushite (3rd through the 7th time-points) and finally (in all the 7th time-point data) to the decrease in the intensities of the most characteristic OCP reflections detected at 4.72°, 9.45° and 9.77° 2θ, in accord with the ICDD PDF 26-1056 for the OCP phase. That decrease in the intensities of the OCP phase could be taken as supporting evidence for the reaction described by Eq. (4), between OCP and CDHA. Performing a reliable Rietveld analysis on the minor phase of OCP was quite difficult, if not impossible at all. If the XRD data were collected over a 2θ range, for instance, only 20–40°, then it could be possible for the researcher to incorrectly assume that brushite would be transforming, for instance, in a *Tris*-SBF solution in 1 week, into apatitic calcium phosphate.[24]

All four solutions used in this study produced the same clear result; the presence of OCP in all the samples even after 1 week of soaking [Fig. 6(d)]. This result is quite strong in the sense that brushite first transforms into OCP in synthetic physiological solutions, and under the experimental conditions of this study, direct transformation of brushite into CDHA-like apatitic calcium phosphate, without first passing through the OCP phase, was not observed.[6] OCP is long regarded as the precursor of bone mineral.[57,58]

Figures 7(a) through 7(f) depict the SEM photomicrographs of brushite powders (sample-1 of Table I) soaked in BM-7, *Lac*-SBF and *Tris*-SBF solutions for 2 d and 1 week. The surfaces of the brushite crystals were smooth and free of nano-crystals, prior to soaking in the solutions [Fig. 2(b)]. BET surface areas of the soaked samples are given in Table III. These SEM micrographs show the transformation products of OCP and CDHA confirmed by the data of Fig. 6. The EDXS data given in Table III pointed out the fact that the BM-3 solution with a Ca/P molar ratio of 1.99 was producing samples with the lowest Ca/P molar ratio, in comparison with the BM-7, *Lac*-SBF and *Tris*-SBF solutions, which all had a Ca/P ratio of 2.50. The theoretical Ca/P ratio of the OCP phase is 1.333, whereas that of CDHA is 1.50. The EDXS data (by being <1.50) of Table III also proved the biphasic nature (i.e., OCP-CDHA) of samples soaked for 1 week in the biomineralization solutions. The experimental data therefore showed that brushite was degrading and transforming itself into calcium phosphates of higher Ca/P molar ratio, with an increase in soaking time at 37°C.

In some of the SEM micrographs [e.g., Figs. 7(a), (c), (d) and (e)] of samples soaked in the biomineralization solutions, the crystals were observed to be hollow. The starting material for the soaking experiments, i.e., Sample-1 of Table I, was ground into a fine powder to crack those WL-type crystals, and then examined with SEM to investigate if the hollow texture was present at the start or developed later during the biomineralization solution soaking experiments. Figure 8 shows the microstructure of the ground sample, together with some debris from the grinding operation. The micrograph of Fig. 8(a) provided clear evidence that the original WL-type brushite crystals were not completely dense. It is apparent that during soaking in the biomineralization solutions the bulk of these crystals (perhaps consisting of a more defective or immature brushite-like phase) could have been emptied with relative ease, as depicted in the Fig. 7 micrographs. The micrograph of Fig. 8(b), on the other hand, depicts that some of the crystals used as the starting material in the soaking experiments of Figs. 5, 6 and 7 were not as hollow as those shown in Fig. 8(a), but the presence of striated layers could still be indicative of compositional changes, as mentioned above in discussing the crystal structure of brushite.

It should be noted that the extent of any hydrothermal transformation of a DCPD-based substance into OCP and CDHA immersed in an aqueous solution shall strongly depend on the overall dimensions or thickness (sizes) of the samples. The current study used micron-size powders and if the samples were bulky and much larger (or much smaller), then the transformation times determined and reported here may not be directly applicable to such different sizes.

Samples 3 through 8 of Table II were synthesized to investigate the influence of small concentrations of Zn^{2+} ions in the brushite synthesis solutions on the resultant crystal morphology. The nominal Zn/Ca solution molar ratios in these experiments were given in Table II. EDXS analyses performed on these samples were not able to detect any Zn in the synthesized samples; ICP-AES would have been the better choice of analysis (instead of EDXS) to determine the

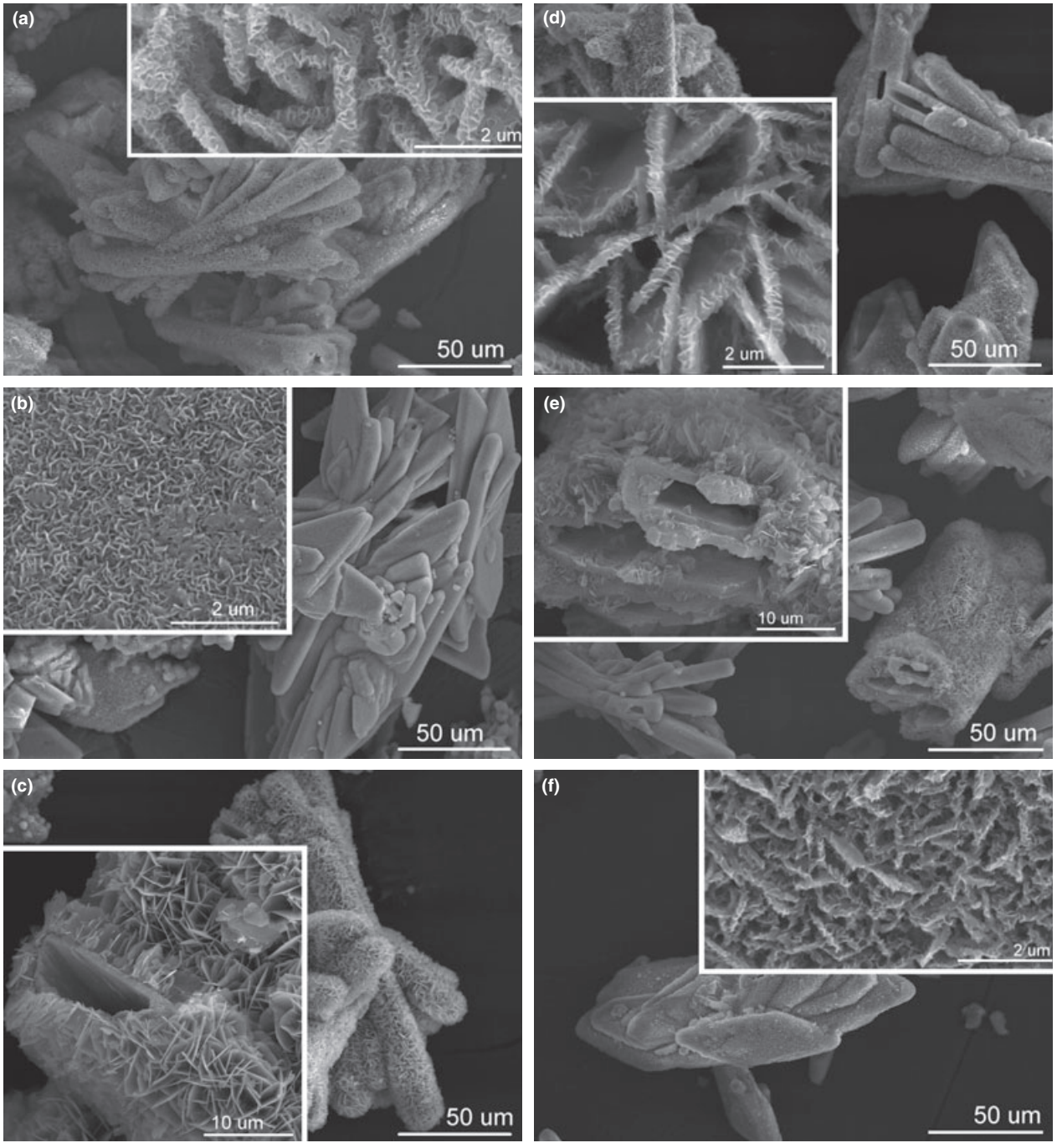

Fig. 7. SEM photomicrographs of sample-1 soaked at 37°C in (a) BM-7 for 2 d, (b) BM-7 for 1 week, (c) *Lac*-SBF for 2 d, (d) *Lac*-SBF for 1 week, (e) *Tris*-SBF for 2 d and (f) *Tris*-SBF for 1 week.

Table III. BET Surface Areas and EDXS Analysis

Sample	Surface area (m^2/g)	Ca/P molar[†]
1	<1	0.97, 0.99
BM-3/1 week	115	1.20, 1.26
BM-7/1 d	–	1.05, 1.14
BM-7/2 d	–	1.26, 1.34
BM-7/1 week	117	1.33, 1.46
Lac-SBF/1 d	–	0.97, 0.99
Lac-SBF/2 d	–	1.15, 1.23
Lac-SBF/1 week	120	1.43, 1.47
Tris-SBF/1 d	–	0.96, 1.00
Tris-SBF/2 d	–	1.13, 1.21
Tris-SBF/1 week	108	1.37, 1.44

[†]Two measurements on each sample.

much smaller amounts of Zn which might have been incorporated into these samples. However, the influence exerted on the crystal morphology of brushite by the Zn^{2+} ions present in the non-agitated, static synthesis solutions was drastic, as shown in the SEM micrographs given in Fig. 9.

The lowest concentration of Zn used during the synthesis of sample-3 [Fig. 9(a)] caused the WL-shaped brushite crystals to acquire the dumbbell-shape, with the thickening of the individual plates of the original WL-shape [in comparison with sample-1 of Fig. 2(b)]. Further increase in the Zn concentration of the synthesis solutions [samples 4 and 5; Figs. 9(b) and (c)] caused the filling of the gaps between the individual plates, and much denser dumbbells of brushite were formed. Those dumbbells progressively turned into more or less spherical granules in samples 6 through 8 [Figs. 9(d) through (f)], with further increase in the Zn con-

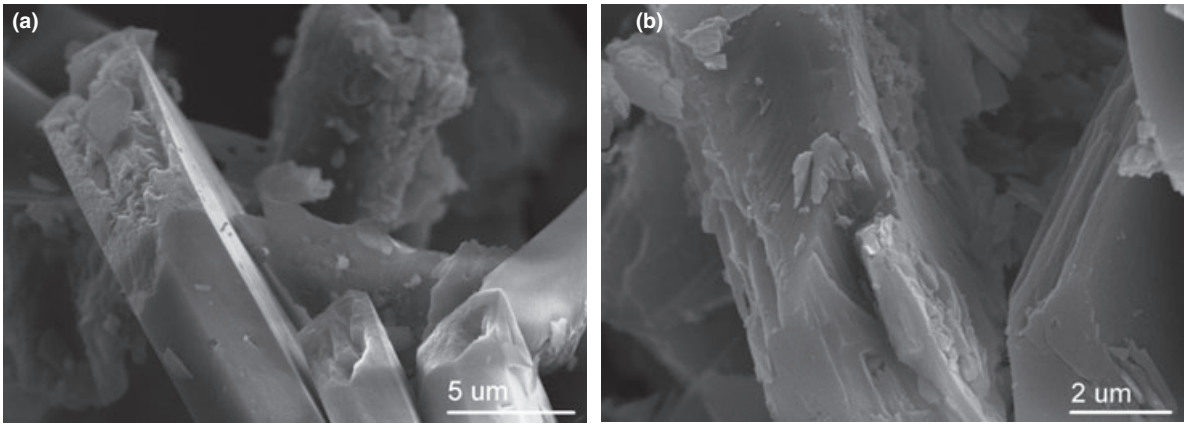

Fig. 8. SEM photomicrographs showing the interiors of sample-1 crystals (after destructive grinding of crystals).

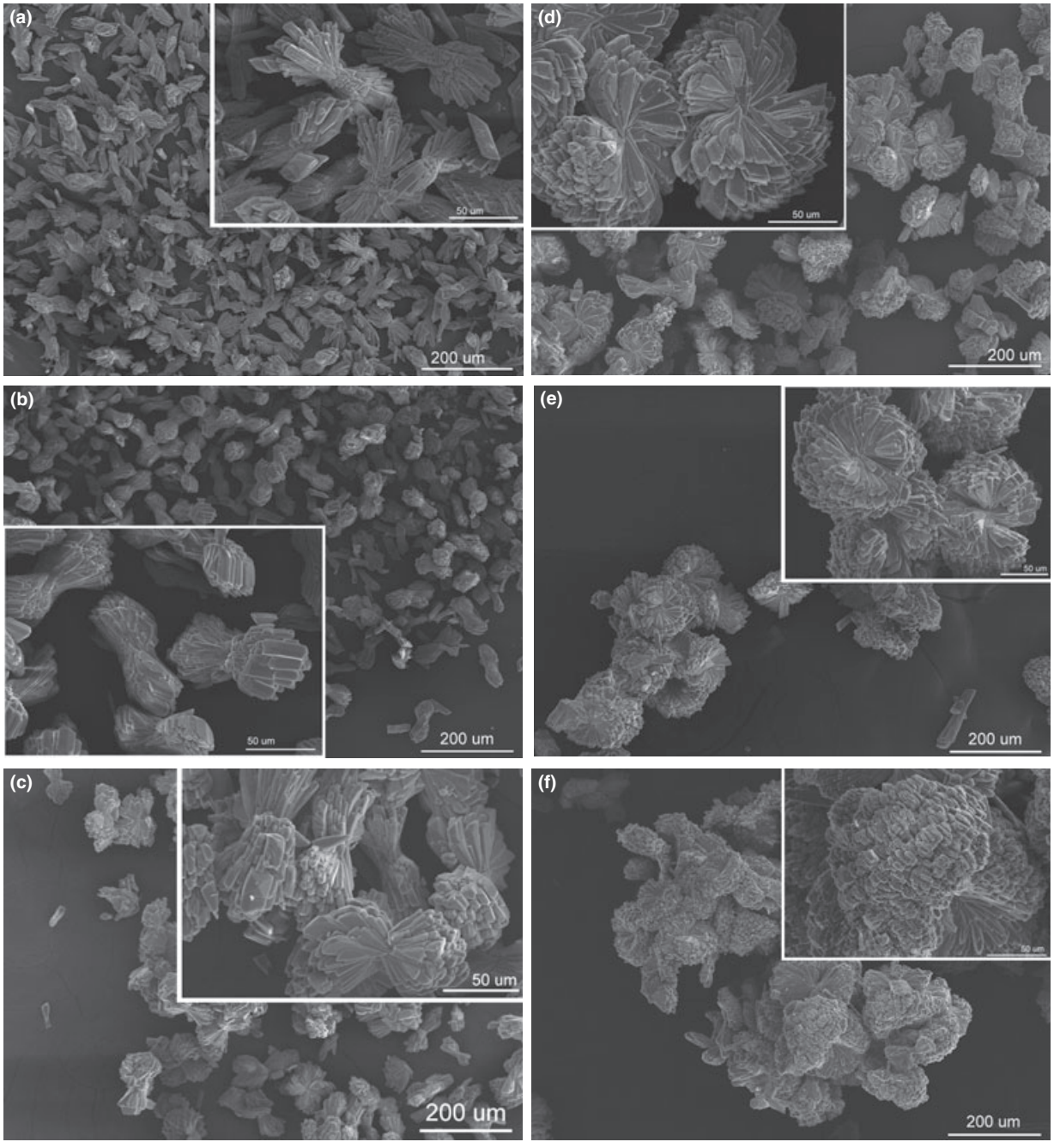

Fig. 9. SEM photomicrographs of (a) sample-3, (b) sample-4, (c) sample-5, (d) sample-6, (e) sample-7 and (f) sample-8 of Table I.

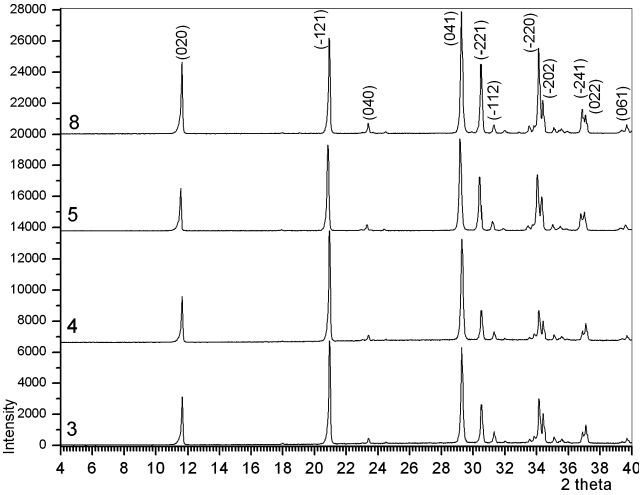

Fig. 10. XRD data of pure brushite samples synthesized at RT in the presence of Zn^{2+} (numbers on traces correspond to sample numbers from Table I).

centration of the synthesis solutions. The mean microgranule size in samples 5 through 8 was around 100 μm. XRD traces given in Fig. 10 showed that the phase of those granules was brushite (conforming to the ICDD PDF 9-0077) with a suppressed intensity of the (020) reflection, quite similar to that shown in Fig. 2(a) for Zn-free sample-1.

Zinc phosphate ($Zn_3(PO_4)_2{\cdot}nH_2O$) cements have been used in dentistry since the late 19th century to join the tooth root to the crown, and the initial phase formed is an acidic and x-ray amorphous zinc phosphate phase.[59,60] Hopeite ($Zn_3(PO_4)_2{\cdot}4H_2O$), on the other hand, is a highly crystalline material and can readily form in aqueous solutions containing dissolved salts of $ZnCl_2$ and ammonium phosphate. The XRD data of samples 3 through 8 did not show any hopeite (Fig. 10).

When we replaced Zn with Mg or Fe (under experimental conditions similar to those of samples 3 through 8), microgranules did not form, only WL-type brushite crystals were obtained. When we added similar amounts of Zn^{2+} ions to the FP-synthesis recipes, such microgranules did not form as well.

Madsen[6] reported that the Zn ion has an inhibitory effect on the brushite crystallization along its (010) face and caused the crystallization of aggregated brushite crystals. Apparently, the presence of Zn ions in the synthesis solutions of this study were resulting in a gradual increase in the surface free energy of the individual platelets making up those thick water lily (WL) [Fig. 9(a)] and dumbbell-shaped brushite [Fig. 9(b)] crystals, and the system was responding to that increase in surface energy by decreasing the available surface area, i.e., crystals acquiring the shape of spherical microgranules [Figs. 9(d)–(f)]. These microgranules (initial BET surface area <1 m^2/g) soaked for 1 week in BM-7 solution (37°C) were found to have a post-soaking BET surface area of 30 m^2/g and largely transformed into an OCP-CDHA biphasic mixture.

It would be worthwhile to note that the syntheses described here were for static, non-agitated crystallization systems, free of any organic substances, and this would render this method of granule production, in the presence of Zn^{2+}, quite economical. Usually granulation processes for calcium phosphate bioceramics require the use of closely-controlled pelletizers and the simultaneous addition of certain benign organics and plasticizers to the initial powder mixtures. The complete removal of those organics may then pose a serious challenge to the engineer, if the biomaterials are to be used in clinical implantation. Our follow-up study on the preparation of these granules will first focus on the determination of the ppm level incorporation of zinc into the resultant brushite microgranules. Such microgranules may find uses in the manufacture of biopolymer-brushite composites.

IV. Conclusions

1. Conventional, flat plate-type brushite crystals were shown to undergo a maturation process during their synthesis, meaning that their Ca/P molar increased from around 0.8 for 80 min of stay in the synthesis solution to around 1 for 24 h of stay in the same.
2. Brushite crystals prepared at room temperature in static crystallization systems containing precipitated calcite and $NH_4H_2PO_4$ as the starting chemicals were found to transform into a biphasic mixture of OCP and CDHA, when soaked for 1 week in different biomineralization solutions (including Tris- and sodium lactate-buffered SBF solutions) at 37°C.
3. Biomineralization solution selected did not change the phase assemblage of the resultant material. Brushite crystals did not directly transform into single-phase apatite in 1 week of soaking time in any of the solutions used in this study.
4. Static soaking of brushite crystals in different biomineralization media always resulted in a significant increase in the BET surface areas of the samples.
5. The presence of small concentrations of Zn^{2+} ions in the brushite synthesis solutions dramatically changed the crystal morphology. Spherical microgranules of brushite were synthesized for the first time in non-agitated, organic-free aqueous systems.

Notes

Certain commercial instruments or materials are identified in this article solely to foster understanding. Such identification does not imply recommendation or endorsement by the authors, nor does it imply that the instruments or materials identified are necessarily the best available for the purpose.

Acknowledgments

Manoj K. Jain took part in this study as a summer student researcher of the OU College of Dentistry for a very limited time, and we are hereby grateful to the financial support provided by J. Dean Robertson Society through its Student Summer Research Program. Authors cordially thank Dr. John Dmytryk (OUHSC) to allow us to use his laboratories. Authors gratefully acknowledge the help of Jonathan Hill, Jeff Westrop and Jordan Williams (OU-Norman) for assistance with BET and XRD measurements. A. C. Tas was a visiting professor in the College of Dentistry of the University of Oklahoma Health Sciences Center (OUHSC) between September 2010 and September 2011.

References

[1]P. W. Brown, "Phase Relationships in the Ternary System $CaO–P_2O_5–H_2O$ at 25°C," *J. Am. Ceram. Soc.*, **75**, 17–22 (1992).
[2]R. I. Martin and P. W. Brown, "Phase Equilibria among Acid Calcium Phosphates," *J. Am. Ceram. Soc.*, **80**, 1263–6 (1997).
[3]E. Boanini, M. Gazzano, and A. Bigi, "Ionic Substitutions in Calcium Phosphates Synthesized at Low Temperature," *Acta Biomater.*, **6**, 1882–94 (2010).
[4]S. V. Dorozhkin and M. Epple, "Biological and Medical Significance of Calcium Phosphates," *Angew. Chem. Int. Ed.*, **41**, 3130–46 (2002).
[5]H. Monma and T. Kamiya, "Preparation of Hydroxyapatite by the Hydrolysis of Brushite," *J. Mater. Sci.*, **22**, 4247–50 (1987).
[6]H. E. L. Madsen, "Influence of Foreign Metal Ions on Crystal Growth and Morphology of Brushite ($CaHPO_4{\cdot}2H_2O$) and its Transformation to Octacalcium Phosphate and Apatite," *J. Cryst. Growth*, **310**, 2602–12 (2008).
[7]K. Furutaka, H. Monma, T. Okura, and S. Takahashi, "Characteristic Reaction Processes in the System Brushite-NaOH Solution," *J. Eur. Ceram. Soc.*, **26**, 543–7 (2006).
[8]C. Oliveira, P. Georgieva, F. Rocha, A. Ferreira, and S. F. de Azevedo, "Dynamical Model of Brushite Precipitation," *J. Cryst. Growth*, **305**, 201–10 (2007).
[9]F. Abbona, F. Christensson, M. F. Angela, and H. E. L. Madsen, "Crystal Habit and Growth Conditions of Brushite, $CaHPO_4{\cdot}2H_2O$," *J. Cryst. Growth*, **131**, 331–46 (1993).

[10]V. S. Joshi and M. J. Joshi, "FTIR Spectroscopic, Thermal and Growth Morphological Studies of Calcium Hydrogen Phosphate Dihydrate Crystals," *Cryst. Res. Technol.*, **38**, 817–21 (2003).
[11]S. Mandel and A. C. Tas, "Brushite ($CaHPO_4{\cdot}2H_2O$) to Octacalcium Phosphate ($Ca_8(HPO_4)_2(PO_4)_4{\cdot}5H_2O$) Transformation in DMEM Solutions at 36.5°C," *Mater. Sci. Eng. C*, **30**, 245–54 (2010).
[12]B. Flautre, C. Maynou, J. Lemaitre, P. van Landuyt, and P. Hardouin, "Bone-Colonization of β-TCP Granules Incorporated in Brushite Cements," *J. Biomed. Mater. Res.*, **63B**, 413–7 (2002).
[13]J. M. Kuemmerle, A. Oberle, C. Oechslin, M. Bohner, C. Frei, I. Boecken, and B. von Rechenberg, "Assessment of the Suitability of a New Brushite Calcium Phosphate Cement for Cranioplasty – An Experimental Study in Sheep," *J. Craniomaxillofac. Surg.*, **33**, 37–44 (2005).
[14]F. Theiss, D. Apelt, B. Brand, A. Kutter, K. Zlinszky, M. Bohner, S. Matter, C. Frei, J. A. Auer, and B. von Rechenberg, "Biocompatibility and Resorption of a Brushite Calcium Phosphate Cement," *Biomaterials*, **26**, 4383–94 (2005).
[15]D. Apelt, F. Theiss, A. O. El-Warrak, K. Zlinszky, R. Bettschart-Wolfisberger, M. Bohner, S. Matter, J. A. Auer, and B. von Rechenberg, "*In Vivo* Behavior of three different Injectable Hydraulic Calcium Phosphate Cements," *Biomaterials*, **25**, 1439–51 (2004).
[16]T. Kokubo, "Surface Chemistry of Bioactive Glass-Ceramics," *J. Non-Cryst. Solids*, **120**, 138–51 (1990).
[17]D. Bayraktar and A. C. Tas, "Chemical Preparation of Carbonated Calcium Hydroxyapatite Powders at 37°C in Urea-Containing Synthetic Body Fluids," *J. Eur. Ceram. Soc.*, **19**, 2573–9 (1999).
[18]R. R. Kumar and M. Wang, "Biomimetic Deposition of Hydroxyapatite on Brushite Single Crystals Grown by the Gel Technique," *Mater. Lett.*, **49**, 15–9 (2001).
[19]S. J. Lin, R. Z. LeGeros, and J. P. LeGeros, "Adherent Octacalcium Phosphate Coating on Titanium Alloy using Modulated Electrochemical Deposition Method," *J. Biomed. Mater. Res.*, **66A**, 819–28 (2003).
[20]H. S. Azevedo, I. B. Leonor, C. M. Alves, and R. L. Reis, "Incorporation of Proteins and Enzymes at Different Stages of the Preparation of Calcium Phosphate Coatings on a Degradable Substrate by a Biomimetic Methodology," *Mater. Sci. Eng. C*, **25**, 169–79 (2005).
[21]J. Pena, I. I. Barba, A. Martinez, and M. Vallet-Regi, "New Method to Obtain Chitosan/Apatite Materials at Room Temperature," *Solid State Sci.*, **8**, 513–9 (2006).
[22]F. Yang, J. G. C. Wolke, and J. A. Jansen, "Biomimetic Calcium Phosphate Coating on Electrospun Poly(Epsilon-Caprolactone) Scaffolds for Bone Tissue Engineering," *Chem. Eng. J.*, **137**, 154–61 (2008).
[23]A. Rakngarm and Y. Mutoh, "Electrochemical Deposition of Calcium Phosphate Film on Commercial Pure Titanium and Ti–6Al–4V in two types of Electrolyte at Room Temperature," *Mater. Sci. Eng. C*, **29**, 275–83 (2009).
[24]A. C. Tas and S. B. Bhaduri, "Chemical Processing of $CaHPO_4{\cdot}2H_2O$: Its Conversion to Hydroxyapatite," *J. Am. Ceram. Soc.*, **87**, 2195–2200 (2004).
[25]J. A. Juhasz, S. M. Best, A. D. Auffret, and W. Bonfield, "Biological Control of Apatite Growth in Simulated Body Fluid and Human Blood Serum," *J. Mater. Sci. Mater. Med.*, **19**, 1823–9 (2008).
[26]N. Temizel, G. Girisken, and A. C. Tas, "Accelerated Transformation of Brushite to Octacalcium Phosphate in New Biomineralization Media Between 36.5° and 80°C," *Mater. Sci. Eng. C*, **31**, 1136–43 (2011).
[27]D. Rohanova, A. R. Boccaccini, D. M. Yunos, D. Horkavcova, I. Brezovska, and A. Helebrant, "Tris Buffer in Simulated Body Fluid Distorts the Assessment of Glass-Ceramic Scaffold Bioactivity," *Acta Biomater.*, **7**, 2623–30 (2011).
[28]M. H. Salimi, J. C. Heughebaert, and G. H. Nancollas, "Crystal Growth of Calcium Phosphates in the Presence of Magnesium Ions," *Langmuir*, **1**, 119 –22 (1985).
[29]A. Bigi, M. Gazzano, A. Ripamonti, and N. Roveri, "Effect of Foreign Ions on the Conversion of Brushite and Octacalcium Phosphate into Hydroxyapatite," *J. Inorg. Biochem.*, **32**, 251–7 (1988).
[30]P. N. Kumta, C. Sfeir, D. H. Lee, D. Olton, and D. Choi, "Nanostructured Calcium Phosphates for Biomedical Applications: Novel Synthesis and Characterization," *Acta Biomater.*, **1**, 65–83 (2005).
[31]D. H. Lee and P. N. Kumta, "Chemical Synthesis and Stabilization of Magnesium Substituted Brushite," *Mater. Sci. Eng. C*, **30**, 934–43 (2010).
[32]S. Cin, E. Unal, A. Pamir, B. Kologlu, and A. O. Cavdar, "Blood Zinc (Plasma, Red Blood Cell) and Insulin-Like Growth Factor-1 in Children from an Impoverished area in Ankara," *J. Trace Elem. Exp. Med.*, **14**, 31–4 (2001).
[33]D. G. Barceloux, "Zinc," *J. Toxicol. Clin. Toxicol.*, **37**, 279–92 (1999).
[34]G. Oner, B. Bhaumick, and R. M. Bala, "Effect of Zinc-Deficiency on Serum Somatomedin Levels and Skeletal Growth in Young Rats," *Endocrinology*, **114**, 1860–3 (1984).
[35]M. Yamaguchi, H. Oishi, and Y. Suketa, "Stimulatory Effect of Zinc on Bone Formation in Tissue Culture," *Biochem. Pharmacol.*, **36**, 4007–12 (1987).
[36]A. C. Tas, "Synthesis of Biomimetic Ca-Hydroxyapatite Powders at 37°C in Synthetic Body Fluids," *Biomaterials*, **21**, 1429–38 (2000).
[37]A. Pasinli, M. Yuksel, E. Celik, S. Sener, and A. C. Tas, "A New Approach in Biomimetic Synthesis of Calcium Phosphate Coatings using Lactic Acid-Na Lactate Buffered Body Fluid Solution," *Acta Biomater.*, **6**, 2282–8 (2010).
[38]S. Cazalbou, C. Combes, D. Eichert, C. Rey, and M. J. Glimcher, "Poorly Crystalline Apatites: Evolution and Maturation *In Vitro* and *In Vivo*," *J. Bone Miner. Metab.*, **22**, 310–17 (2004).
[39]J. Arsic, D. Kaminski, P. Poodt, and E. Vlieg, "Liquid Ordering at the Brushite-010-Water Interface," *Phys. Rev. B*, **69**, 245406 (2004).
[40]N. A. Curry and D. W. Jones, "Crystal Structure of Brushite, Calcium Hydrogen Orthophosphate Dihydrate: A Neutron Diffraction Investigation," *J. Chem. Soc. A*, **23**, 3725–9 (1971).
[41]ICDD PDF: International Centre for Diffraction Data Powder Diffraction File; Newtown Square, Pennsylvania (www.icdd.com).
[42]A. C. Tas, "A New Calcium Phosphate Cement Composition and a Method for the Preparation Thereof"; U.S. Patent No: 6,929,692 August 16, 2005.
[43]J. Redepenning and J. P. McIsaac, "Electrocrystallization of Brushite Coatings on Prosthetic Alloys," *Chem. Mater.*, **2**, 625–7 (1990).
[44]J. Redepenning, T. Schlessinger, S. Burnham, L. Lippiello, and J. Miyano, "Characterization of Electrolytically Prepared Brushite and Hydroxyapatite Coatings on Orthopedic Alloys," *J. Biomed. Mater. Res.*, **30**, 287–94 (1996).
[45]L. Y. Huang, K. W. Xu, and J. Lu, "A Study of the Process and Kinetics of Electrochemical Deposition and the Hydrothermal Synthesis of Hydroxyapatite Coatings," *J. Mater. Sci. Mater. Med.*, **11**, 667–73 (2000).
[46]A. Ince, N. Schutze, C. Hendrich, R. Thull, J. Eulert, and J. F. Lohr, "*In Vitro* Investigation of Orthopedic Titanium and Brushite-Coated Titanium Surfaces Using Human Osteoblasts in the Presence of Gentamycin," *J. Arthroplasty*, **23**, 762–71 (2008).
[47]E. A. Abdel-Aal, D. Dietrich, S. Steinhaeuser, and B. Wielage, "Electrocrystallization of Nanocrystallite Calcium Phosphate Coatings on Titanium Substrate at Different Current Densities," *Surf. Coat. Technol.*, **202**, 5895–900 (2008).
[48]C. Combes, C. Rey, and M. Freche, "XPS and IR Study of Dicalcium Phosphate Dihydrate Nucleation on Titanium Surfaces," *Colloids Surf., B*, **11**, 15–27 (1998).
[49]A. C. Tas, "Electroless Deposition of Brushite ($CaHPO_4{\cdot}2H_2O$) Crystals on Ti–6Al–4V at Room Temperature," *Int. J. Mater. Res.*, **97**, 639–44 (2006).
[50]E. Busenberg and L. N. Plummer, "A Comparative study of the Dissolution and Crystal Growth Kinetics of Calcite and Aragonite," *U.S. Geol. Surv. Bull.*, **1578**, 139–68 (1986).
[51]O. W. Duckworth and S. T. Martin, "Dissolution Rates and Pit Morphologies of Rhombohedral Carbonate Minerals," *Am. Mineral.*, **89**, 554–63 (2004).
[52]P. Cubillas, S. Kohler, M. Prieto, C. Chairat, and E. H. Oelkers, "Experimental Determination of the Dissolution Rates of Calcite, Aragonite, and Bivalves," *Chem. Geol.*, **216**, 59–77 (2005).
[53]R. K. Tang, M. Hass, W. Wu, S. Gulde, and G. H. Nancollas, "Constant Composition Dissolution of Mixed Phases II. Selective Dissolution of Calcium Phosphates," *J. Colloid Interface Sci.*, **260**, 379–84 (2003).
[54]I. V. Dolgaleva, I. G. Gorichev, A. D. Izotov, and V. M. Stepanov, "Modeling of the Effect of pH on the Calcite Dissolution Kinetics," *Theor. Found. Chem. Eng.*, **39**, 614–21 (2005).
[55]A. C. Tas, "Monetite ($CaHPO_4$) Synthesis in Ethanol at Room Temperature," *J. Am. Ceram. Soc.*, **92**, 2907–12 (2009).
[56]G. Montes-Hernandez, F. Renard, N. Geoffroy, L. Charlet, and J. Pironon, "Calcite Precipitation from CO_2-H_2O-$Ca(OH)_2$ Slurry under High Pressure of CO_2," *J. Cryst. Growth*, **308**, 228–36 (2007).
[57]M. Iijima and Y. Moriwaki, "Effects of Ionic Inflow and Organic Matrix on Crystal Growth of Octacalcium Phosphate; Relevant to Tooth Enamel Formation," *J. Cryst. Growth*, **198/199**, 670–6 (1999).
[58]O. Suzuki, "Octacalcium Phosphate: Osteoconductivity and Crystal Chemistry," *Acta Biomater.*, **6**, 3379–87 (2010).
[59]L. Herschke, J. Rottstegge, I. Lieberwirth, and G. Wegner, "Zinc Phosphate as Versatile Material for Potential Biomedical Applications Part I," *J. Mater. Sci. Mater. Med.*, **17**, 81–94 (2006).
[60]L. Herschke, I. Lieberwirth, and G. Wegner, "Zinc Phosphate as Versatile Material for Potential Biomedical Applications Part II," *J. Mater. Sci. Mater. Med.*, **17**, 95–104 (2006). □